Electrooxidation Mechanisms and Discharge Characteristics of Borohydride on Different Catalytic Metal Surfaces

Hua Dong, Ruixiang Feng, Xinping Ai, Yuliang Cao, Hanxi Yang,* and Chuansin Cha

Department of Chemistry, Wuhan University, Wuhan 430072, PR China

Received: January 18, 2005; In Final Form: April 7, 2005

The electrooxidation behavior of BH_4^- on electrocatalytic Pt, hydrolytically active Ni, and noncatalytic Au electrodes were comparatively reexamined and a more generalized reaction mechanism was proposed to explain the very different anodic properties of BH_4^- on the different metal electrodes. In this mechanism, the anodic reaction behavior of BH_4^- are determined by a pair of conjugated reactions: electrochemical oxidation and chemical hydrolysis of BH_4^-, the relative rates of which depend on the anodic materials, applied potentials, and chemical states of the anodic surfaces. At Pt surface, the electron number of BH_4^- oxidation increases with the increased potential polarization, while the actual electron number of BH_4^- oxidation on Ni electrode is 4 at most due to the poor electrocatalytic activity of the oxidized Ni surface and the strong catalytic activity of metallic Ni for chemical recombination of the adsorbed H intermediate. On the hydrolytic−inactive Au surface, the anodic reaction of BH_4^- can proceed predominately through direct electrochemical oxidation, delivering a near 8e discharge capacity.

1. Introduction

Direct borohydride fuel cells (DBFC) with aqueous borohydride solutions as liquid fuels have attracted considerable research interest in recent years due to their higher theoretical voltage, higher hydrogen storage density, and faster anodic kinetics in comparison with hydrogen or methanol fuel cells.[1−4] A severe problem encountered in developing DBFC is the simultaneous hydrolysis of BH_4^- ions at anodic surfaces along with their electrochemical oxidation, which not only makes the actual electrochemical capacity much less than the expected 8-electron oxidation for an BH_4^- ion, but also brings some difficulties in the design and safety managements of the cells due to the accumulation of H_2 evolved.

Since DBFC was first proposed in the early 1960s, the anodic oxidation and concomitant hydrolysis reaction of BH_4^- have been extensively studied on a number of metal surfaces and several reaction mechanisms have been suggested to explain the very different anodic behavior of BH_4^- oxidation on different metal anodes.[5−11] In earlier studies, Indig and Snyder[5] reported a 4e anodic reaction of BH_4^- on a porous nickel electrode. At that time, Elder and Hickling[12] found that the columbic number of BH_4^- on a Pt electrode is between 2 and 4, and Kubokawa et al.[13] found a 6e oxidation reaction on a Pd-coated carbon electrode. Amendola et al.[1] reported a 7e reaction on an Au electrode. Recently, a number of research groups reexamined the anodic oxidation processes of BH_4^- and also found that the anodic oxidation of BH_4^- may proceed through different paths, as a multielectron reaction process, depending on different experimental conditions such as applied electrode potential, pH values of solution, and anodic materials.[2−4,10,11] Nevertheless, the underlying chemistry of BH_4^- electrooxidation is still not fully revealed.

To enhance the utilization of BH_4^- as an anodic fuel, it is of primary importance to clarify the factors affecting the reaction mechanisms of the electrochemical oxidation and the associated hydrolysis of BH_4^-. In this paper, we chose three types of typical metals (Ni, Pt, Au) representing the catalytically active, moderate, and inactive anodes, and comparatively investigated the electrooxidation behavior and discharge characteristics of BH_4^-. This work was aimed at obtaining a deeper understanding of the reaction mechanism of BH_4^- electrooxidation so as to help in solving the technical problems currently encountered in the development of DBFC with high efficiency.

2. Experimental Section

2.1. Reagents and Electrodes. KBH_4 (AR, 95% purity, Shanghai, China) and KOH (GR, 85% purity, Shanghai, China) were used as received and all solutions were prepared with doubly distilled water. Unless otherwise mentioned, the electrolyte used in this study was a 25 g/L of KBH_4 + 1 mol/L of KOH solution.

The Ni electrode employed in our experiments was a porous sintered Ni plate. To eliminate the oxides on the surface of Ni electrode, cathodic polarization treatment was carried out for 30 min in 1 mol/L of KOH solution before each experiment. Pt/C (XC-72) catalyst was prepared by chemical precipitation of H_2PtCl_6 with alkaline BH_4^- solution and then washed with distilled water. After the solution was dried in a vacuum at 120 °C, Pt/C powders were fabricated with Teflon binder into a membrane (Pt/C:Teflon = 90:10) and Pt loading was estimated to be ca. 0.2 mg/cm^2 by subtracting the PTFE and carbon contents from the catalyst membrane.

2.2. Electrochemical Measurements. Cyclic voltammograms (CV) of BH_4^- on Ni and Pt electrodes were measured with a three-electrode system with use of an electrochemical workstation (CHI660a, Shanghai, China). The Ni working electrode was a Ni rode (ϕ 0.5 mm) sealed in a Teflon tube and the Pt working electrode was a microdisk Pt electrode (ϕ 0.1 mm) fabricated by sealing a Pt wire in a glass tube with one end exposed to electrolyte. The counter electrode was a large sheet of Ni mesh and the reference electrode was an Hg/HgO electrode. All the experiments were carried out at room temperature (~25 °C).

* Address correspondence to this author. Phone: +86-27-68754526. Fax: +86-27-87884476. E-mail: ece@whu.edu.cn.

10.1021/jp050322v CCC: $30.25
Published on Web 05/04/2005

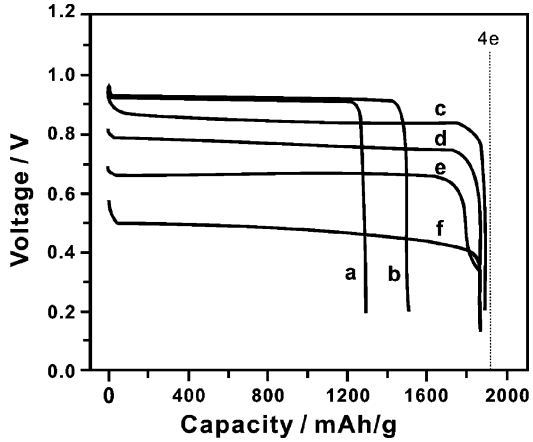

Figure 1. The discharge curves of a KBH_4−air cell at various currents, using Ni (15 cm^2) as the electrocatalytic anode and MnO_2 as the electrocatalytic cathode: (a) 20, (b) 50, (c) 100, (d) 150, (e) 200, and (f) 300 mA.

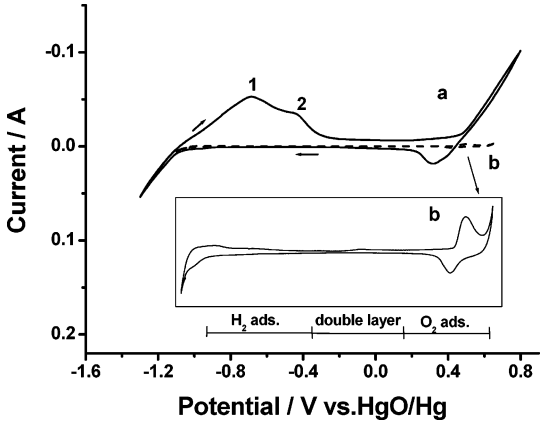

Figure 2. Cyclic voltammograms (CV) of a Ni electrode in (a) 25 g/L of KBH_4 + 1 mol/L of KOH solution and (b) 1 mol/L of KOH solution. Sweep rate: 10 mV/s. The potential scan started from open circuit potential and continued to +0.8 V.

Discharge behavior of KBH_4 were examined in prototype KBH_4−air cells, using MnO_2 as a cathode catalyst. The prototype air cell was made from a rectangular polymethyl methacrylate cell (L 5 cm × W 1.5 cm × H 6 cm) with a square hole (W 3 cm × H 5 cm) hollowed out on one sidewall and covered with air cathode membrane. The test metal anodes were generally a 6 cm^2 area and directly inserted into the cell container ca. 1 cm away from the air electrode. The air electrodes used in this work consisted of a catalyst layer and a gas diffusion layer. The catalyst layer was a 0.1 mm thick membrane containing the MnO_2 catalyst (20 wt %) loaded on activated carbon (65 wt %) and poly(tetrafluoroethylene) (PTFE) binder (15 wt %). The gas diffusion layer was prepared by mixing acetylene black (60 wt %) and PTFE emulsion (40 wt %) with 2-propanol to form a paste and then rolling the paste into a 0.5 mm thick film. Both the catalyst and gas diffusion layers were pressed together with a nickel mesh in between at 80 kg/cm^2 and sintered at 270 °C in air for a half hour to remove organic residues. Since MnO_2 has sufficient electrocatalytic activity for oxygen reduction and has no catalytic activity for the electrooxidation and hydrolysis of BH_4^- ion, we can thus calculate the actual electron numbers of BH_4^- by discharge capacity of the KBH_4−air cells.

3. Results and Discussion

3.1. Electrooxidation Behavior of BH_4^- on Ni Anode. Figure 1 gives the discharge curves of a KBH_4−Air cell at various currents with Ni and MnO_2 as electrocatalytic anode and cathode, respectively. It can be seen from the figure that the discharge capacity of 1 g of KBH_4 is ca. 1290 mAh at the current drain of 20 mA and increases to 1500 mAh when the discharge current rises to 50 mA, showing a simultaneous increase of discharge capacity with discharge currents. However, once the current increases to higher than 100 mA, the discharge capacity remains almost at the same value of ca. 1860 mAh.

To understand these unusual discharge behavior, we measured the discharge potentials of the Ni electrode at various currents and found that the potential of the Ni anode was always more negative than the potential of the standard hydrogen electrode (SHE, −0.93 V vs Hg/HgO) in alkaline solution at the current below 50 mA, whereas the discharge potential were more positive than −0.93 V at the current of more than 100 mA. This implies that the electrochemical reduction of water and the hydrolysis of BH_4^- may take place during the discharge process at a potential more negative than −0.93 V, which unavoidably consumes a portion of the BH_4^- ions to form H_2 and therefore reduces the number of BH_4^- ions available for electrochemical oxidation. Further discussion on the two-coupled reactions is given later in the paper. In comparison, since the discharge of the Ni anode at 20 mA showed a more negative potential and took a longer discharge time than at 50 mA, the hydrolysis of BH_4^- may proceed faster and longer at the lower discharge current, and accordingly, the lower electrochemical capacity of BH_4^- was observed at the lower discharge rates. Another question needed to be answered in Figure 1 is the observation of almost the same 4e oxidation capacity for BH_4^- cells discharged at the currents ⩾100 mA. At these discharge currents, the anodic potentials were found to be much more positive than −0.93 V, and therefore BH_4^- could not hydrolyze and should deliver their 8e capacity in the electrooxidation reactions. However, we can only obtain a 4e reaction capacity for all the BH_4^- cells with the Ni catalyzed anode and still observe H_2 generation from the Ni electrode at discharge currents ⩾100 mA. These experimental phenomena seem to clarify the fact that the electrochemical oxidation of BH_4^- on the Ni electrode can only proceed through a 4e reaction, involving H_2 generation produced from the discharge rather than from hydrolysis of BH_4^-. Thus, the total anodic reaction of BH_4^- on the Ni electrode can be expressed as:[3,11]

$$BH_4^- + 4OH^- \rightarrow BO_2^- + 2H_2O + 2H_2 + 4e \qquad (1)$$

Figure 2 depicts the CV curves of BH_4^- on the Ni electrode in 1 mol/L of KOH solution. The main CV features of BH_4^- electrooxidation are the two peaks at ca. −0.68 and −0.42 V in the initial anodic scan. Unlike the CV curves of BH_4^- on Pt and Au electrodes,[10] no anodic peak is observed in the reverse scan, suggesting that BH_4^- has no electrochemical activity on the oxidized Ni surface once it is scanned to the positive potential region >0 V. In a previous study of BH_4^- electrooxidation on the Ni electrode,[14] Tsionskii et al. suggested from the data from the liner polarization method that BH_4^- is electrochemically inactive in the potential range between −0.9 and −0.4 V and the anodic response is due to the electrochemical oxidation of adsorbed H atoms generated from the catalytic hydrolysis of BH_4^-. The CV peaks (1 and 2 in Figure 2) for BH_4^- electrooxidation are indeed located in the potential region of H adsorption on the Ni electrode, apparently in agreement with Tsionskii's suggestion. However, since the hydrolysis reaction of BH_4^- can only occur at a more negative potential than −0.93 V and the oxidation peaks (1 and 2) in Figure 2 are

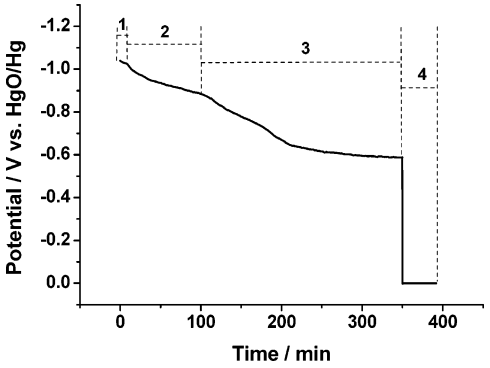

Figure 3. The potential changes of a Ni electrode in alkaline KBH_4 solution (1) at open-circuit, (2) after adding a drop of 0.1% TU every 20 min, (3) at rest when H_2 generation was ceased, and (4) discharged at 1 mA.

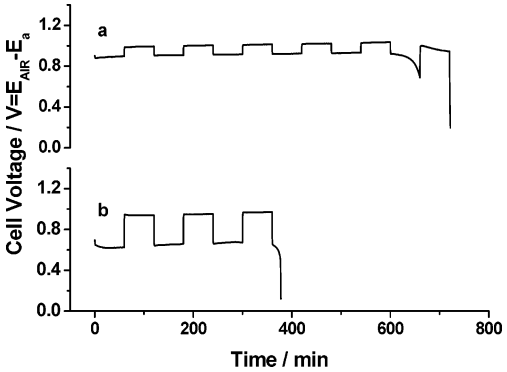

Figure 4. The intermittent discharge curves of a Ni electrode in 0.5 g of KBH_4 + 20 mL of 2 mol/L of KOH solution at two different currents: (a) 50 and (b) 200 mA. The cell voltages were measured as $E_{air} - E_a$.

always observable even at the anodic scan with initial potential more positive than −0.93 V, it is thus reasonable to assign the CV peaks to the adsorbed H atoms produced by the electrooxidation of BH_4^- ions rather than those generated by the hydrolysis reaction of BH_4^- ions.

To further confirm this assignment, we used $(NH_2)_2CS$ (TU) as an additive to "poison" the active H adsorption sites on the Ni electrode and then monitored the potential changes of the Ni anode to see the effect of adsorbed hydrogen on the anodic behavior of BH_4^- ions. This is because thiourea is known to be a strong adsorbing poison that replaces adsorbed hydrogen from the electrode surfaces and strongly decreases the activity of electrodes for the hydrogen evolution reaction from water electroreduction.[15,16] As is shown in Figure 3, the open-circuit potential (OCP) of the Ni electrode is −1.06 V, which is more negative than the SHE in alkaline solution. At this stage, BH_4^- hydrolyzes fiercely with severe evolution of hydrogen gas. With the addition of TU, the electrode potential is positively shifted and the H_2 evolution rate is decreased gradually. When the potential is shifted to be more positive than −0.93 V, we cannot visualize any H_2 gas to evolve from the anodic surface, indicating the cutoff of BH_4^- hydrolysis by addition of TU. At this stage, even without further addition of TU, the potential of the Ni electrode is still increased continuously and finally kept at a stable value of ca. −0.6 V. If the cells are discharged even at a very small current of 1 mA, the potential of the Ni anode immediately climbed to 0 V, showing a rapid loss of catalytic activity of the Ni electrode for the electrooxidation of BH_4^- in the presence of TU. This suggests that BH_4^- electrooxidation cannot proceed on the Ni electrode if the hydrogen adsorption is inhibited. In fact, this conclusion seems to support, to some extent, the previous inference on the BH_4^- electrooxidation proposed by Lee et al.[2] that the BH_4^- electrooxidation reaction takes place through stepwise dissociative adsorption of hydrogen such as

$$BH_n(OH)_{4-n}^- \rightarrow BH_{n-1}^-(OH)_{4-n}^- + H \quad (2)$$

$$BH_{n-1}(OH)_{4-n}^- + OH^- \rightarrow BH_{n-1}(OH)_{5-n}^- + e \ (n = 4, 3, 2, 1) \quad (3)$$

To obtain an insight into the correlation between the hydrolysis and electrooxidation reactions of the BH_4^- ion, we adopted the intermittent-discharge method to estimate the H_2 generation rates at various discharge rates. Figure 4 shows the intermittent-discharge curve of the BH_4^- ion on the Ni anode. Since no hydrolysis of BH_4^- happens on the Ni electrode at the current of 200 mA and the total electron number for BH_4^- electrooxidation is 4 at this condition, we can calculate from Figure 4b the hydrolysis rate of BH_4^- at rest to be 3.14 mAh/min by subtracting the actual discharge capacity from the theoretical capacity of the BH_4^- ions added. Furthermore, we can also calculate the hydrogen generation rate in the period of BH_4^- discharge from Figure 4a by use of the hydrolysis rate of BH_4^- (3.14 mAh/min), since the Ni anode used for measurements of the discharge curves in Figure 4 is the same electrode. Such a simple calculation reveals that the hydrogen generation rate on the discharged Ni anode is 1.14 mAh/min at 50 mA, which is much lower than that at open circuit (3.14 mAh/min) and much higher than that at a high rate discharge of 200 mA (∼0 mAh/min). This potential-dependent hydrolysis of BH_4^- implies that the hydrolysis process must involve the electrochemical reduction of H_2O, and most likely the BH_4^- hydrolysis is the consequence of a pair of coupled reactions of BH_4^- electrooxidation and H_2O electoreduction, i.e.

$$BH_4^- + 2OH^- \rightarrow BH_3(OH)^- + H_2O + 2e \quad (4)$$

$$2H_2O + 2e \rightarrow 2OH^- + H_2 \quad (5)$$

$$BH_4^- + H_2O \rightarrow BH_3(OH)^- + H_2 \quad (6)$$

In fact, the experimental facts seem to indicate that the electrooxidation process of BH_4^- is always accompanied by its coupling reaction of H_2O electroreduction, in which the rate of H_2O electroreduction is potential dependent. Thus, the reaction mechanism of BH_4^- electrooxidation on the Ni anode could be well explained in that at open-circuit, the apparent potential of an BH_4^- electrode is a mixed potential determined by eqs 4 and 5.

When the anodic potential is moved toward the positive direction during discharge, the electroreduction rate of H_2O decreases and H_2 evolution slows down correspondingly. Once the potential rises up to higher than SHE, H_2O cannot be reduced on the anodic surface and, as a result, the anodic reaction of the BH_4^- electrode proceeds predominately through the mechanism shown in eq 4. In fact, eq 4 can be written in two steps

$$BH_4^- + OH^- \rightarrow BH_3(OH)^- + H + e \quad (4a)$$

$$H + OH^- \rightarrow H_2O + e \quad (4b)$$

$$\text{or } 2H \rightarrow H_2 \quad (4b')$$

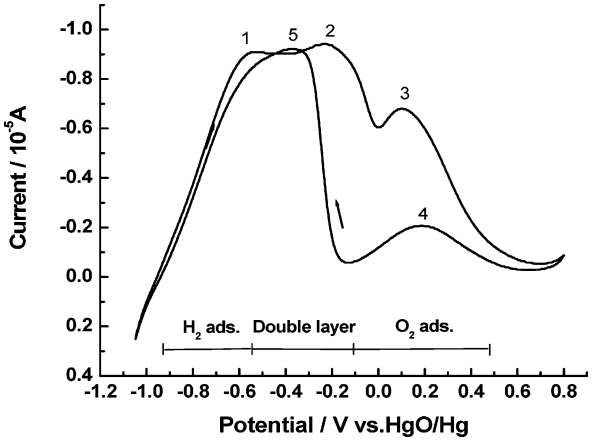

Figure 5. CV curves of a Pt electrode in 1 mol/L of KOH solution containing 0.5 g of KBH_4. Sweep rate: 50 mV/s.

At he Ni surface, the catalytic recombination of 2H into gaseous H_2 is well-known to be a kinetically favorable reaction (eq 4b′) and therefore the H atoms produced at the first step of BH_4^- electrooxidation (eq 4a) are preferably to become H_2 evolved rather than to be further oxidized through the electrochemical step (eq 4b). Thus, it is not surprising that the H_2 generation is always observed during the process of BH_4^- electrooxidation even at the more positive potentials. Analogously, if the oxidation reaction of an BH_4^- ion involves four dissociation steps on the Ni anode such as eqs 2−3, 4H must be chemically recombined into gaseous H_2 in total, and as a result, the maximum discharge capacity for an BH_4^- ion can only be a 4e oxidation capacity, as observed in Figure 1.

3.2. Electrooxidation Behavior of BH_4^- on Pt Electrodes. A typical CV curve of BH_4^- on the Pt electrode in alkaline solution is given in Figure 5, which generally shows three oxidation peaks (peak 1, 2, 3) on the positive scan, a single oxidation peak at +0.2 V (peak 4), and an overlapped oxidation band (peak 5) on the reverse negative scan. In previous work,[10] peaks 1 and 2 were attributed to the electrooxidation of H and BH_3OH^-, respectively, which were formed in the catalytic hydrolysis of BH_4^-, and peak 3 was assigned to the direct oxidation of BH_4^-. However, if the anodic peaks 1 and 2 arise from the hydrolysis products H and BH_3OH^-, the currents of these peaks would increase remarkably as long as the scanning is paused at the beginning potential for a longer time to accumulate a sufficient amount of the intermediates. Failure to observe this phenomenon implies that there must be some different mechanism responsible for the CV behavior of BH_4^- electrooxidation observed in Figure 5. Taking into account that there are three different types of surface states on the Pt electrode, i.e., H-adsorption region, double-layer region, and O-adsorption region, in the potential range of BH_4^- electrooxidation (−1.0 to +0.4 V), it is possible that the CV features in Figure 5 represent different reaction processes of BH_4^- on the different chemical states of the Pt surface.

Figure 6 compares the CV behavior of BH_4^- on clean and TU-poisoned Pt surfaces. As shown in Figure 6, once the Pt electrode adsorbs TU molecules, only one single oxidation peak is observed at a very positive potential of +0.2 V and other CV peaks observable at more negative potentials from the clean Pt surface all vanished. This indicates that in the region of H-adsorption, BH_4^- electrooxidation must involve the participation of adsorbed H atoms on the Pt surface, whereas at the potential region of surface oxide formation, BH_4^- can be directly oxidized without the need of surface H species. These inferences are supported by the discharge results as shown in Figure 7. It

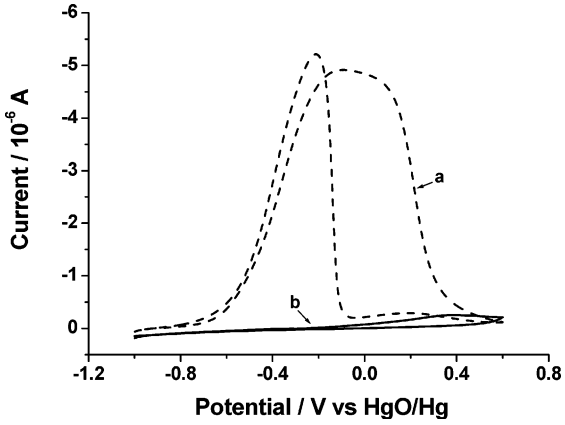

Figure 6. CV curves of a Pt electrode in 1 mol/L of KOH solution containing 0.5 g of KBH_4 and 0.01 g of TU. Sweep rate: 10 mV/s.

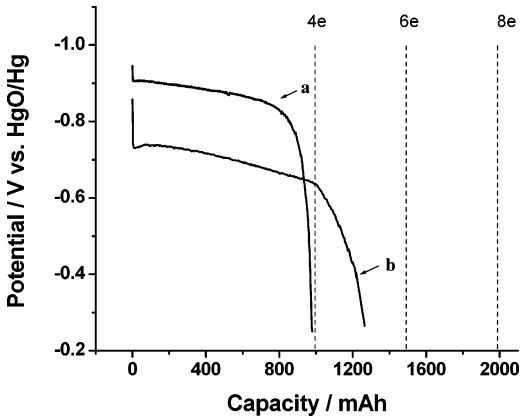

Figure 7. Discharge curves of a Pt/C electrode in 0.5 g of KBH_4 + 1 mol/L of KOH solution at a current density of (a) 25 and (b) 50 mA/cm^2.

can be seen from the figure that the capacity of KBH_4 on the Pt/C electrode is ca. 1960 mAh/g, corresponding to a 4e reaction, at the current density of 25 mA/cm^2. When the current density increases to 50 mA/cm^2, the discharge capacity attains ca. 2600 mAh/g, approaching a 5e oxidation capacity. Since the potentials of the Pt/C electrode at 25 and 50 mA/cm^2 were both more more positive than −0.93 V, the difference in the discharge capacities and electron number cannot be interpreted to be due to the hydrolysis of BH_4^-, and also cannot be explained only from the increased electrochemical polarization. Thus, it seems that the positively shifted potential changes the surface states of the Pt/C electrode and thereby alters accordingly the mechanism of BH_4^- electrooxidation.

The potential changes of the Pt/C electrode at various surface states (Figure 8) also agree with the above suggestion. As can be seen, the OCP of the Pt/C electrode appears to be ca. −0.96 V, more negative than SHE, and at this condition, there is an obvious H_2 evolution on the Pt/C electrode as in the case of the Ni electrode. With dropwise addition of TU to poison the H-adsorption sites of the Pt/C electrode, the electrode potential was found to gradually increase with alleviated H_2 generation. When the potential reached −0.93 V, the H_2 evolution disappeared as expected, suggesting that the BH_4^- hydrolysis is a conjugated reaction between BH_4^- electrooxidation and H_2O electroreduction. However, different from the Ni electrode, BH_4^- electrooxidation can still proceed on the Pt/C electrode in the presence of TU, indicating that the electrooxidation of BH_4^- on the Pt/C electrode can take place in a different mechanism, which does not need the participation of surface H atoms. Particularly, the discharge capacity of BH_4^- on a Pt/C anode

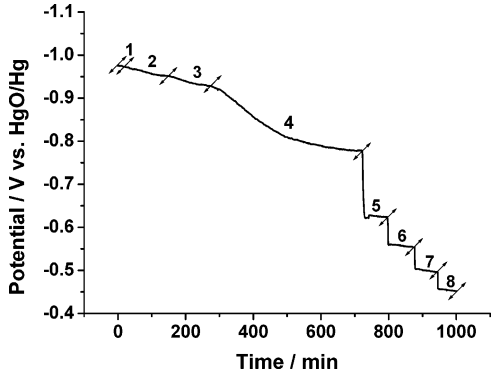

Figure 8. The potential changes of a Pt/C (0.2 mg/cm^2) electrode in 0.5 g of KBH_4 + 1 mol/L of KOH solution with addition of TU: (1) at OCP; (2) after adding a drop of 0.1% TU every 5 min; (3) after adding two drops of 0.1% TU every 5 min; (4) at rest when H_2 generation was ceased on the electrode surface; and discharging at (5) 2.5, (6) 10, (7), and (8) 30 mA/cm^2.

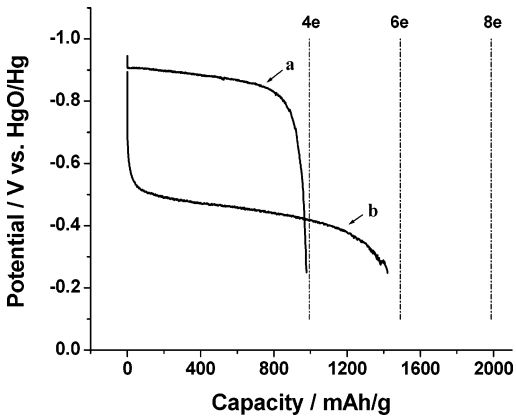

Figure 9. Discharge curves of a Pt/C electrode at 25 mA/cm^2 in (a) 0.5 g of KBH_4 + 1 mol/L of KOH and (b) 0.5 g of KBH_4 + 1 mol/L of KOH + 5×10^{-4} mol/L of TU.

corresponds to a 6e oxidation in the presence of TU, much large than the 4e oxidation capacity obtained at the absence of TU (Figure 9), although the discharge plateau is ca. 0.4 V lower in the presence of TU. This can only be explained by the fact that the adsorption of TU on the Pt/C electrode blocks the reaction route of BH_4^- electrooxidation through adsorbed H intermediate due to the increased polarization. Consequently, the positively shifted potentials greatly facilitate the direct 8e electrooxidation of BH_4^- as previously reported in ref 10.

It should be mentioned that though the experimental results were obtained from a Pt/C electrode, the conclusion drawn above is also valid for the pure Pt electrode, because we found, from comparative measurements of BH_4^- electrooxidation on the carbon anode, that the carbon power showed almost no catalytic activities for the electrooxidation and hydrolysis of BH_4^-, acting only as an inert catalyst carrier.

3.3. Electrooxidation Behavior of BH_4^- on Au Electrodes. Au belongs to a group of metals of high hydrogen overpotential, at which the formation of surface hydrides or hydrogen adsorption are thought to be heavily frustrated. Thus, the selection of Au as an electrocatalyst for the BH_4^- anode may avoid the hydrolysis of BH_4^- and therefore facilitate the complete oxidation of BH_4^-. In the early 1990s, Bard et al. studied the BH_4^- oxidation at the Au electrode by linear voltammetry and estimated the electron number of BH_4^- oxidation to be 8.[8] Recently, Amendola et al. investigated the discharge behavior of $NaBH_4$−air cells and found that the number of electrons utilized per BH_4^- ion was ca. 7.[1]

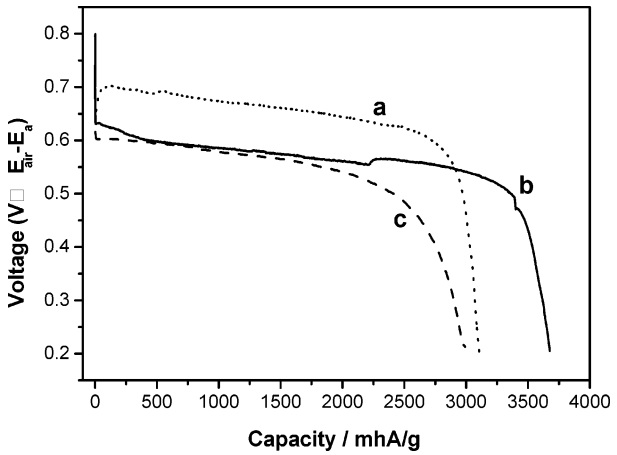

Figure 10. Discharge curves of an Au/C anode in 0.5 mol/L of KBH_4 + 2 mol/L of KOH. The cell voltages were measured as $E_{air} - E_a$.

Figure 10 shows the discharge curves of a prototype−air cell, using an Au-loaded carbon anode. It can be seen that the discharge capacities of BH_4^- attain 3700 g and 3500 mAh/g of KBH_4 at the discharge rate of 1 and 2.5mA/cm^{-2}, corresponding to a delivery of 7.5 and 7.0 electrons per BH_4^- ion, compared with the theoretical capacity predicted from a total 8-electron oxidation of an BH_4^- ion. These results seem to indicate that it is possible to construct a highly efficient DBFC cell with Au or Au alloys.

3.4. A Generalized Model for BH_4^- Electrooxidation. Although a number of investigations have been done in the past and several working mechanisms have been proposed to explain the different oxidation behavior of BH_4^-, a well-accepted model for BH_4^- electrooxidation has not been reached yet. At the present, there are two typical models separately used for an explanation of the experimental phenomena observed from Ni and Pt anodes. One is the stepwise oxidation mechanism proposed by Lee et al.[2] in which BH_n^- dissociates in four steps (n = 4, 3, 2, 1) into an H atom and a BH_{n-1}^- ion, and the resulting BH_{n-1}^- ions combine with OH^- to form $BH_{n-1}(OH)^-$ with release of one electron at each step, as expressed in eqs 2 and 3. This model can well account for the observed 4e oxidation reaction on Ni and the correlation of BH_4^- electrooxidation with H adsorption.

Another different mechanism was suggested by Elder and Hickling,[12] which emphasizes that BH_4^- electrooxidation and hydrolysis reactions take place competitively in two parallel reaction routes depending on the electrode potential. According to this mechanism, BH_4^- electrooxidation could be a predominant reaction in some reaction steps while BH_4^- hydrolysis occurs dominantly in other steps. Although this parallel reaction mechanism can well explain the higher discharge capacity of BH_4^- on the Pt electrode at higher discharge potential, it is difficult to explain how these two parallel reactions can proceed independently in the whole potential region, particularly, how the very active discharge intermediates such as $BH_3(OH)^-$ and $BH_2(OH)^-$ can avoid being hydrolyzed and how BH_4^- ions can still hydrolyze at very positive potentials.

On the basis of the previously documented data[2,10−14] and our experimental evidence discussed above, we think that the electrochemical properties of the BH_4^- anode are determined by a pair of conjugated reactions: BH_4^- electrooxidation and BH_4^- hydrolysis. The rates of these two reactions depend not only on the anodic potential, but also on the chemical states of the anodic surfaces. The overall reaction processes of the BH_4^- anode can be expressed as:

$$BH_n(OH)_{4-n}^- + 2OH^- \rightarrow BH_{n-1}(OH)_{5-n}^- + H_2O + 2e \quad (n = 4, 3, 2, 1) \quad (7)$$

$$BH_n(OH)_{4-n}^- + H_2O \rightarrow BH_{n-1}(OH)_{5-n}^- + H \quad (n = 4, 3, 2, 1) \quad (8)$$

At OCP conditions, no net current passes through the anodic−electrolyte interface and therefore the only reaction on the anode is the hydrolysis of BH_4^- (eq 8). In fact, this hydrolysis reaction can be regarded as a pair of coupled reactions of BH_4^- electrooxidation and H_2O electoreduction as represented by eqs 4 and 5. In the cases of Pt and Ni anodes, these two types of the reactions (eqs 4 and 5) can proceed simultaneously and therefore a notable hydrogen evolution can be observed from the anodic surfaces at the OCP potentials, because of the low overpotential of these two metals for hydrogen formation. When discharging, the anodic behavior of BH_4^- electrooxidation on Pt and Ni electrodes is likewise given rise by the combined action of reactions eq 7 and 8, and which one of these two reactions dominates depends on the potential and chemical states of the anodic surfaces. In the case of the Pt anode, when the discharging potential is shifted to a more positive region, the positively charged anodic surface would greatly accelerate the BH_4^- oxidation (eq 7) and depress the hydrolysis of BH_4^- (eq 8). This may explain a near 8e oxidation of BH_4^- observed from the Pt anode at larger polarization. The only observation of $\leq$4e oxidation capacities for BH_4^- on the Ni surface even at high polarization may result for two reasons: One reason is the greater tendency of the Ni surface to form a surface layer of oxides at less negative potentials, and the BH_4^- electrooxidation is prohibited on the oxidized Ni surface. Another reason is the strong catalytic activity of the Ni surface for chemical recombination of adsorbed H atoms, interrupting the further oxidation of the reaction intermediate. In contrast, due to the high overpotential of hydrogen on the Au surface, the electrochemical reduction of H_2O proceeds with difficulty and accordingly the hydrolysis reaction of BH_4^- cannot take place on the Au anode even at the OCP conditions. As a result, the anodic reaction ofBH_4^- on the Au anode can proceed mainly through the electrochemical oxidation as given by eq 8, delivering a discharge capacity close to 8e oxidation.

4. Conclusions

In this work, we comparatively studied the electrooxidation behavior of BH_4^- on three typical (Pt, Ni, and Au) electrodes and proposed a more generalized model to explain very well the very different behavior of BH_4^- electrooxidation obtained from different electrodes. The main conclusions drawn from this study are as follows:

(1) The anodic behavior of BH_4^- is determined by a pair of conjugated reactions of BH_4^- electrooxidation and hydrolysis, the rates of which depend on the electrode potential, material properties, and chemical states of the anodes.

(2) The electron number of BH_4^- electrooxidation on the Pt electrode increases with the increased potential polarization and can attain complete 8e oxidation at large polarization, while the actual electron number of BH_4^- electrooxidation on the Ni electrode is 4 at most due to the poor electrocatalytic activity of the oxidized Ni surface at positive polarization and the strong catalytic activity of metallic Ni for chemical recombination of the adsorbed H intermediate. On the hydrolytic−inactive Au surface, the anodic reaction of BH_4^- can proceed predominately through direct electrochemical oxidation, leading to a very high utilization of the reaction electrons of BH_4^- ions.

(3) The BH_4^- hydrolysis can be effectively depressed by use of the electrolyte additives, such as TU, to poise the active sites of hydrogen adsorption, which helps to increase the Coulombic efficiency of the anodic reaction of BH_4^- ions.

Acknowledgment. The authors gratefully acknowledge the financial support by the National 973 program of China (Grant No. 2002CB211800)

References and Notes

(1) Amendola, S. C.; Onnerud, P.; Kelly, M. T.; Petillo, P. J.; Sharp-Goldman, S. L.; Binder M. *J. Power Sources* **1999**, *84*, 130.
(2) Lee, S. M.; Kim, J. H.; Lee, H. H.; Lee, P. S.; Lee. J. Y. *J. Electrochem. Soc.* **2002**, *149*, A603.
(3) Li, Z. P.; Liu, B. H.; Arai, K.; Suda, S. *J. Electrochem. Soc.* **2003**, *150*, A868.
(4) Liu, B. H.; Li, Z. P.; Suda, S. *J. Electrochem. Soc.* **2003**, *150*, A398.
(5) Indig, M. E.; Snyder. R. N. *J. Electrochem. Soc.* **1962**, *109*, 1104.
(6) Jasinski, R. *Electrochem. Technol.* **1965**, *3*, 40.
(7) Morris, J. H.; Gysling, H. J.; Reed, D. *Chem. Rev.* **1985**, *85*, 51.
(8) Mirkin, M. V.; Bard. A. J. *Anal. Chem.* **1991**, *63*, 532.
(9) Mirkin, M. V.; Yang, H.; Bard. A. J. *J. Electrochem. Soc.* **1992**, *139*, 2212.
(10) Gyenge, E. *Electrochim. Acta* **2004**, *49*, 965.
(11) Liu, B. H.; Li, Z. P.; Suda, S. *Electrochim. Acta* **2004**, *49*, 3097.
(12) Elder, J. P.; Hickling. A. *Trans. Faraday Soc.* **1962**, *58*, 1852.
(13) Kubokawa, M.; Yamashita, M. Abe, K. *Denki Kagaku* **1968**, *36*, 788.
(14) Tsionskii, M. V.; Ivanov, M. V. *Russ. J. Electrochem.* **1989**, *257*, 64.
(15) Subranyam, P. K. In *Comprehensive Treatise of Electrochemistry*; Bockris, J. O'M., Conway, B. E., Yeager, E. B. ,White, R. E., Eds.; Plenum Press: New York, 1981; Vol. 4, Chapter 8, p 411.
(16) Gao, L.; Conway, B. E. *Electrochim. Acta* **1994**, *39*, 1681